

# Aerodynamic Predictions, Comparisons, and Validations Using Missile DATCOM (97) and Aeroprediction 98 (AP98)

Thomas J. Sooy\* and Rebecca Z. Schmidt†

*Technology Service Corporation, Silver Spring, Maryland 20910*

The U.S. Air Force Missile DATCOM (97 version) and the Naval Surface Warfare Center Dahlgren Division Aeroprediction 98 (AP98) are two widely used aerodynamic prediction codes. These codes predict aerodynamic forces, moments, and stability derivatives as a function of angle of attack and Mach number for a wide range of axisymmetric and nonaxisymmetric missile configurations. This study evaluates the accuracy of each code compared to experimental wind-tunnel data for a variety of missile configurations and flight conditions. The missile configurations in this study include axisymmetric body alone, body wing tail, and body tail. The aerodynamic forces under investigation were normal force, pitching moment, axial force, and center-of-pressure location. For the configurations detailed in this paper, these case studies show normal force prediction for both codes to have minimal error. Both AP98 and Missile DATCOM were effective in predicting pitching-moment coefficients, though at times limiting factors were necessary. Finally, both AP98 and DATCOM predict reasonable axial-force coefficients for most cases, though AP98 proved more accurate for the body-wing-tail and body-tail configurations evaluated in this study.

## Nomenclature

$C_A$	= axial-force coefficient
$C_m$	= pitching-moment coefficient
$C_N$	= normal-force coefficient
$l_b$	= length of body (calibers)
$M_\infty$	= Mach number
$Re$	= Reynolds number
$S_r$	= sum of the squares of the residuals between the error at each data point and the mean error
$s_y$	= rms error
$X_{CP}$	= center-of-pressure location nondimensionalized by calibers
$y_i$	= error at each data point
$\alpha$	= angle of attack
$\phi$	= roll angle from vertical ( $\phi = 0$ deg is + configuration)

## I. Introduction

THE 1997 Version of the U.S. Air Force Missile DATCOM<sup>1</sup> and the Naval Surface Warfare Center Dahlgren Division (NSWC/DD) Aeroprediction 98 (AP98)<sup>2,3</sup> are semi-empirical aerodynamic prediction codes that calculate aerodynamic forces, moments, and stability derivatives as a function of angle of attack and Mach number for a variety of axisymmetric and nonaxisymmetric missile configurations. Both codes have the added capability to predict pressure contours and interference factors as well as the capability for the user to easily substitute and/or change aerodynamic parameters to fit specific applications for a broad range of flight conditions. Flight conditions and aerodynamic parameters range from subsonic to hypersonic speeds, angles of attack up to 90 deg, and control surface deflections from  $-35$  to  $35$  deg. The output computes fin-alone, body-alone, and body + finset aerodynamic forces

and moments in addition to center-of-pressure location, interference factors, and geometric data. The capabilities of each aeroprediction code are very comprehensive.

There are key features in each code that make them both attractive for a user to produce a robust aerodynamic analysis of a missile system. Missile DATCOM has extensive trim capabilities and the ability to numerically model a configuration by inserting experimental data. DATCOM also has the ability to model airfoils in more detail including both user definition and a NACA airfoil database. Additionally, Missile DATCOM has the capability to develop aerodynamic data for airbreathing systems. AP98's features include a plotting program for aerodynamic coefficients as well as a geometric sketch of the input configuration. AP98 also has improved axial-force coefficient prediction capability and produces both structural loading and aerothermal output.

This validation effort was conducted to determine the accuracy of each code for specific missile types when compared to wind-tunnel data. Other studies have been extended to compare AP98 and DATCOM with computational fluid dynamics (CFD) codes and experimental wind-tunnel data.<sup>4</sup> The following case studies are representative of a variety of missile configurations that include axisymmetric body alone, body tail, and body wing tail at various flight conditions. Missiles with inlets were not studied in this validation effort because AP98's prediction capability does not yet extend to airbreathing systems. Normal forces, pitching moments, axial forces, and center-of-pressure location were compared with experimental results.

## II. Details

The flight conditions and geometry for the configurations presented in this paper are shown in Table 1. Unless otherwise noted, all cases are modeled with untrimmed fin data, 0-deg fin deflections and 0-deg roll (+ configuration). Boundary layers were modeled as either turbulent or naturally transitioning in Missile DATCOM. AP98 has four separate boundary-layer options. A turbulent boundary layer in Missile DATCOM corresponded to the "Model with Boundary Layer Trip" option in AP98. A naturally transitioning boundary layer in DATCOM corresponded to one of two separate options in AP98: "Typical Flight Configuration" or "Smooth Model With No Boundary Layer Trip." The second-order shock expansion method was implemented in DATCOM for all cases at supersonic speeds above Mach 2.0 in accordance with Ref. 5. Aerodynamic forces were calculated with either full or zero base drag as specified for each case. Unless otherwise noted, the reference length

Presented as Paper 2004-1246 at the AIAA 42nd Aerospace Sciences Meeting, Reno, NV, 5–8 January 2004; received 22 January 2004; revision received 8 March 2004; accepted for publication 21 April 2004. Copyright © 2004 by Technology Service Corporation. Published by the American Institute of Aeronautics and Astronautics, Inc., with permission. Copies of this paper may be made for personal or internal use, on condition that the copier pay the \$10.00 per-copy fee to the Copyright Clearance Center, Inc., 222 Rosewood Drive, Danvers, MA 01923; include the code 0022-4650/05 \$10.00 in correspondence with the CCC.

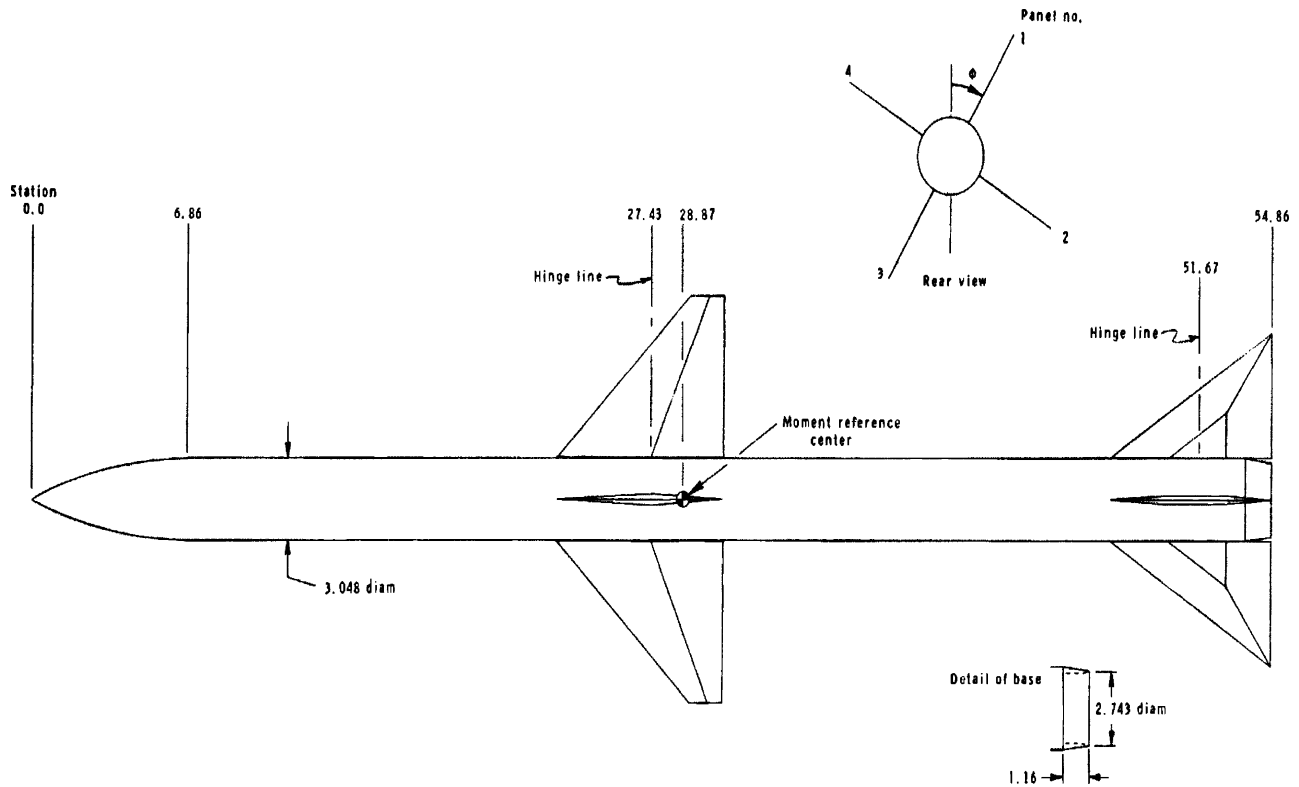
\*Weapons Systems Engineer, Missile and Threat Systems Department, 962 Wayne Avenue, Suite 800.

†Weapons Systems Engineer, Missile and Threat Systems Department, 962 Wayne Avenue, Suite 800. Life Member AIAA.

**Table 1 Configuration geometry/flight conditions**

Case number	Mach number	Reynolds number <sup>a</sup>	Boundary layer	Base drag	Roll angle, deg	Reference length <sup>a</sup>	Reference area <sup>a</sup>	$X_{CG}$ <sup>a</sup>
1	1.5 4.6	$8.2 \times 10^6$ per meter	Turbulent	Full	45	3.048 cm	7.30 cm <sup>2</sup>	28.9 cm
2	2.0	$0.7 \times 10^6$ per foot	Turbulent	Full	0	1.0 m	0.79 m <sup>2</sup>	8.0 m
3	2.01	$2.0 \times 10^6$ per foot	Natural	Zero	0	3.0 in.	7.07 in. <sup>2</sup>	15 in.
4	2.01	$2.0 \times 10^6$ per foot	Natural	Zero	0	3.0 in.	7.07 in. <sup>2</sup>	15 in.
5	2.01	$2.0 \times 10^6$ per foot	Natural	Zero	0	3.0 in.	7.07 in. <sup>2</sup>	15 in.
6	1.42 3.08	$2.0 \times 10^6$ per foot	Natural	Full	0	3.0 cm	7.07 cm <sup>2</sup>	27.0 cm

<sup>a</sup>Units in all cases are preserved from references.

**Fig. 1 Body-wing-tail configuration.**<sup>7</sup>

and reference area values correspond to the missile diameter and cross-sectional area, respectively.

The rms error is given by Eq. (1) (Ref. 6) with  $n$  equal to the total number of data points:

$$s_y = \sqrt{\sum (y_i - \bar{y})^2 / n} \quad (1)$$

where

$$\bar{y} = \sum \frac{y_i}{n} = \sum \left[ \left( \frac{x_{\text{exp}_i} - x_{\text{theory}_i}}{x_{\text{exp}_i}} * 100 \right) / n \right] \quad (2)$$

All aerodynamic coefficient error is calculated using Eq. (1) and (2) at intervals of 5-deg angle of attack from 0 deg to the maximum angle of attack for each case. Errors quoted in this paper represent rms error over the entire angle-of-attack range. All center-of-pressure location ( $X_{cp}$ ) data are plotted in calibers from the c.g. reference location, with positive values reflecting a location aft of the c.g. The difference between experimental and predicted  $X_{cp}$  with respect to body length in calibers was calculated for any angle of attack by

Eq. (3):

$$X_{cp}/l_b = \{[(X_{cp})_{\text{theory}} - (X_{cp})_{\text{exp}}]/l_b\} \text{calibers} \quad (3)$$

All experimental center-of-pressure data not presented in the references were nondimensionalized by calibers and calculated using Eq. (4). At zero angle of attack, experimental  $X_{cp}$  was set equal to DATCOM's predicted  $X_{cp}$  as a reference point:

$$(X_{cp})_{\text{exp}} = -C_m/C_N \quad (4)$$

### III. Results

#### A. Case 1: Wing-Body-Tail Configuration

The first case considered for validation is a body-wing-tail configuration similar to a Sparrow III type missile.<sup>7</sup> The configuration, shown in Fig. 1, has a tangent-ogive nose, two fin sets consisting of four panels, and a moment reference location just aft of the wing hinge line. Both the wing and tail fin sets, depicted in

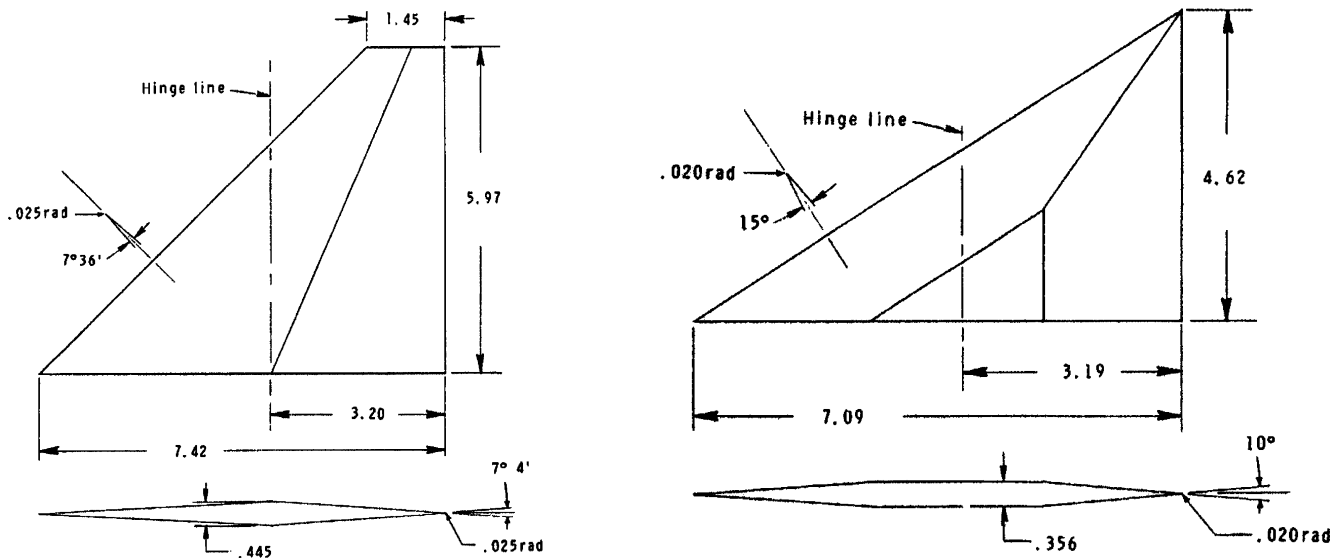
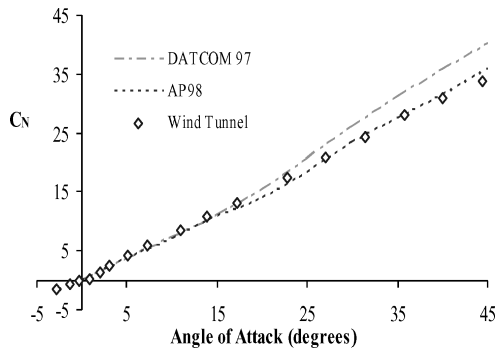
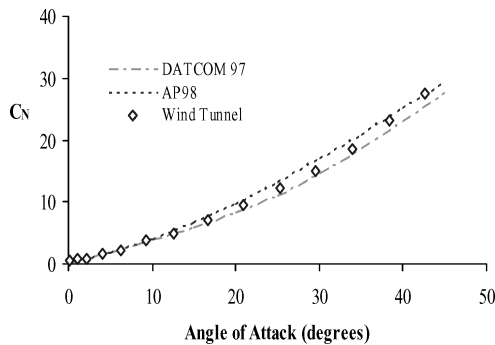
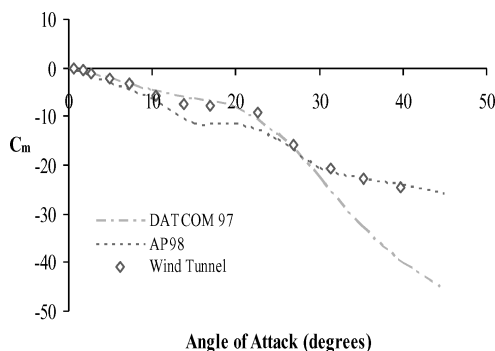
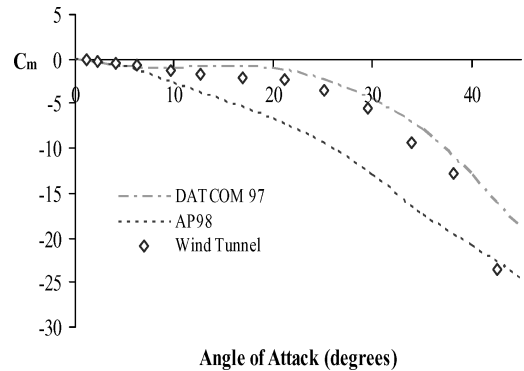
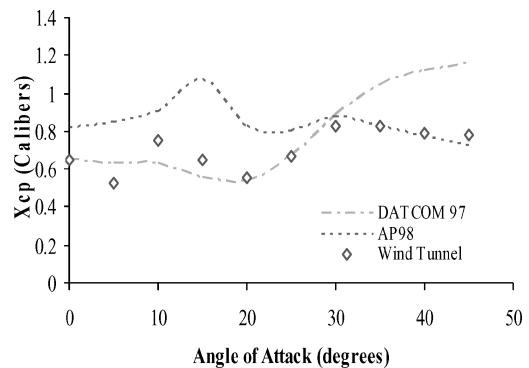
Fig. 2 Wing and tail-fin airfoil and geometry.<sup>7</sup>Fig. 3  $C_N$  vs  $\alpha$ ,  $M_\infty = 1.5$ ,  $\phi = 45$  deg.Fig. 4  $C_N$  vs  $\alpha$ ,  $M_\infty = 4.6$ ,  $\phi = 45$  deg.Fig. 5  $C_m$  vs  $\alpha$ ,  $M_\infty = 1.5$ ,  $\phi = 45$  deg.Fig. 6  $C_m$  vs  $\alpha$ ,  $M_\infty = 4.6$ ,  $\phi = 45$  deg.Fig. 7  $X_{CP}$  vs  $\alpha$ ,  $M_\infty = 1.5$ ,  $\phi = 45$  deg.

Fig. 2, are of high aspect ratio and assumed to be of constant tapering thickness. A turbulent boundary layer and full base drag conditions were assumed. The study was conducted over an angle of attack range from 0 to 45 deg; Mach numbers 1.5, 2.0, 2.35, 2.87, and 4.6; 0-deg fin deflection, 0- and 45-deg roll angles; and a Reynolds number of  $8.2 \times 10^6$  per meter. The results presented for this case are Mach numbers 1.5 and 4.6 at 45-deg roll. It was determined that the reference length was the length of the missile.

As shown in Fig. 3 and 4, the variation of normal-force coefficients with angle of attack is reasonably linear for the test conditions.<sup>7</sup> The normal-force coefficient results for both codes are

in agreement with the experimental data with less than 9% error for DATCOM and 7% for AP98. Additional studies of normal force at Mach numbers 2.0, 2.35, and 2.87 proved that both codes provide comparatively accurate results.

The pitching-moment coefficients for this configuration show variability between the two codes. Figures 5 and 6 present the pitching-moment coefficients vs angle of attack. In Fig. 5, the results for DATCOM are in agreement up to approximately 30-deg

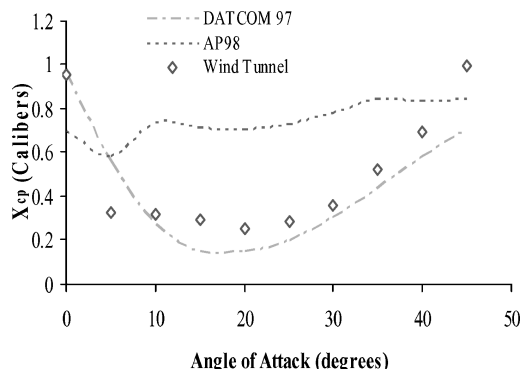


Fig. 8  $X_{CP}$  vs  $\alpha$ ,  $M_\infty = 4.6$ ,  $\phi = 45$  deg.

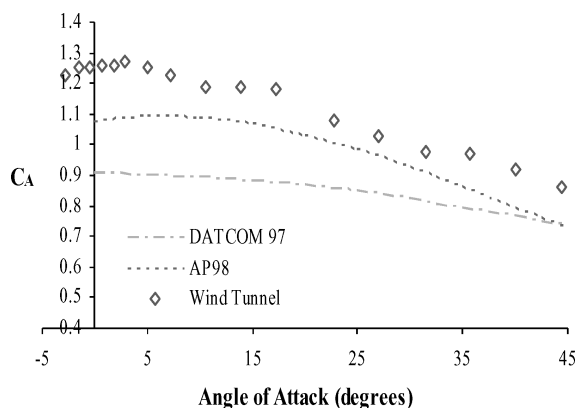


Fig. 9  $C_A$  vs  $\alpha$ ,  $M_\infty = 1.5$ ,  $\phi = 45$  deg.

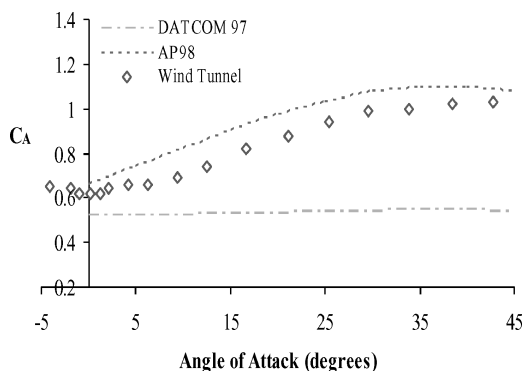


Fig. 10  $C_A$  location vs  $\alpha$ ,  $M_\infty = 4.6$ ,  $\phi = 45$  deg.

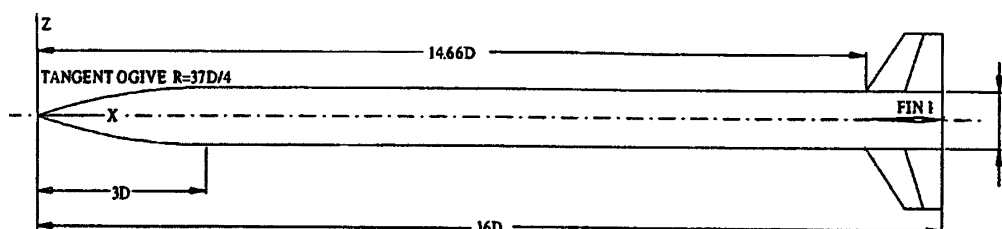


Fig. 11 Body-tail configuration.<sup>8</sup>

angle of attack, with a 12% error in this range. AP98 maintains the trend of wind-tunnel data with the largest errors occurring between 10- and 30-deg angle of attack. Limiting the angle-of-attack range to 15 deg in Fig. 5 gives errors of 11% for DATCOM and 22% for AP98. In Fig. 6, DATCOM more closely follows the trend of the wind-tunnel data, while AP98 produces significantly larger errors above approximately 5-deg angle of attack. Limiting the angle of attack to 15 deg for this case gives errors of 36% error for DATCOM and 61% for AP98.

$X_{CP}$  is independent of reference location, whereas the predicted moment coefficient is highly dependent on this location. Therefore, comparison of pitching-moment coefficients should also include an examination of center-of-pressure location. Predicted  $X_{CP}$  presents a more reliable measure of code accuracy, which can help to determine whether erratic moment coefficient results are linked to possible difficulty in code prediction or simply a scaling factor as a result of user-specified reference location. Figures 7 and 8 show the results of  $X_{CP}$  in calibers from the center of gravity. In Fig. 7, the percent error of  $X_{CP}/l_b$  is less than two for both DATCOM and AP98 at any given angle of attack. DATCOM produces more accurate results in Fig. 8 with a percent error of  $X_{CP}/l_b$  less than two at any given angle of attack. AP98 error for this condition is less than 3%.

Figures 9 and 10 are the axial-force coefficient comparisons for  $\phi = 45$  deg at Mach 1.5 and 4.6. DATCOM shows discrepancy in axial force, especially at the higher Mach number, where it appears it can be calculating  $C_A$  independent of angle of attack. The errors for DATCOM in Fig. 9 and 10 are 4 and 12%, respectively. AP98 more closely follows the trend of the experimental data with errors of 3% for Fig. 9 and 5% for Fig. 10.

Axial force and drag are the most difficult of aerodynamic forces to predict. There are several components that have a combined effect

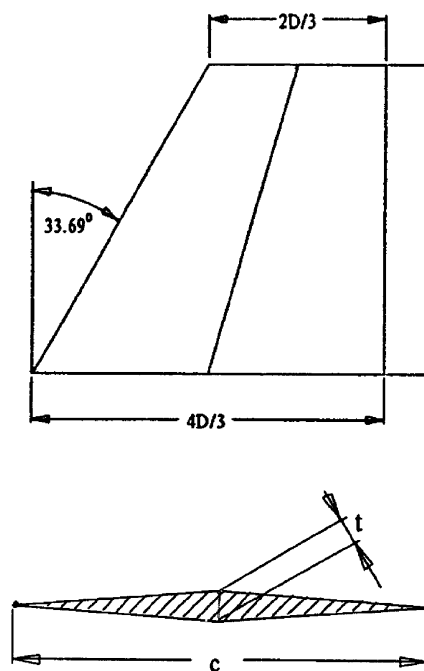


Fig. 12 Tail-fin and airfoil geometry.<sup>8</sup>

on the total drag; they are skin-friction drag (also known as viscous drag), wave drag, and base drag. These components are affected by factors including configuration geometry, freestream Mach number, Reynolds number, angle of attack, and body roughness. Considering how difficult axial-force prediction can be, AP98 results show the code's capability in predicting axial force within  $\pm 10\%$  error. Based on these results, it is concluded that AP98 produces accurate axial-force coefficients for a body-wing-tail configuration with high-aspect-ratio wings.

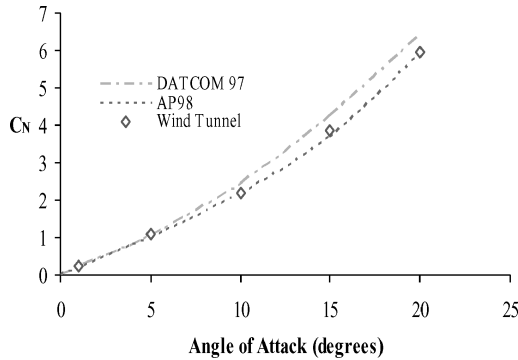


Fig. 13  $C_N$  vs  $\alpha$ ,  $M_\infty = 2.0$ ,  $\phi = 0$  deg.

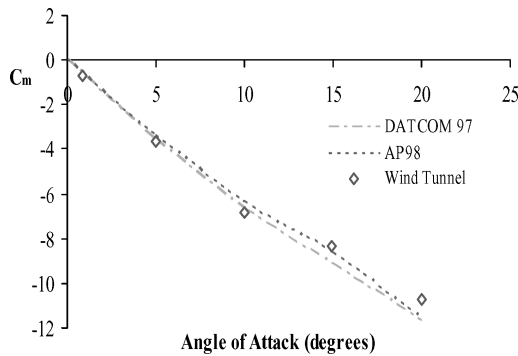


Fig. 14  $C_m$  vs  $\alpha$ ,  $M_\infty = 2.0$ ,  $\phi = 0$  deg.

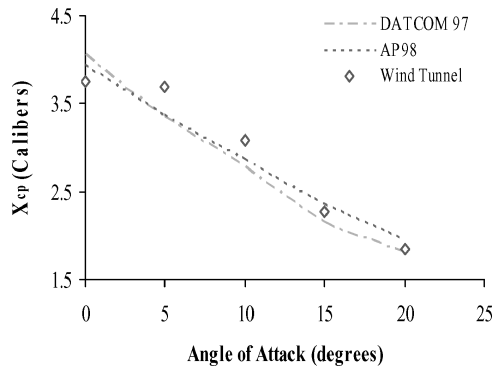


Fig. 15  $X_{CP}$  Location vs  $\alpha$ ,  $M_\infty = 2.0$ ,  $\phi = 0$  deg.

## B. Case 2: Body-Tail Configuration

The next configuration considered for validation is a conventional body-tail missile.<sup>8</sup> The missile, shown in Fig. 11, has a three-caliber tangent-ogive nose with four tail fins arranged in a cruciform pattern. Each fin has a leading-edge sweep angle of  $33.69$  deg and a diamond-shaped airfoil, as shown in Fig. 12. A thickness-to-chord ratio of  $0.07$  is maintained across the entire span of each fin. The moment reference location is  $L/2$  ( $8D$ ). The tests were conducted at Mach  $2.0$ , a Reynolds number of  $0.7 \times 10^6$  per foot, and a turbulent boundary layer.

The results, shown in Figs. 13–15, demonstrate that the aero-prediction codes are in agreement with respect to normal force, pitching moment, and center-of-pressure location for this type of configuration. For normal-force coefficients, Missile DATCOM predicted these values with a 4% error, and AP98 predicted these values with a 3% error. Predicted pitching-moment coefficients for DATCOM had a 4% error and AP98 data had a 3% error. Finally, center-of-pressure location was predicted with a maximum error of 2% for DATCOM and AP98 at any given angle of attack.

## C. Case 3: Body-Alone Configuration

The next missile evaluated is a body-alone configuration shown in Fig. 16 (Refs. 9 and 10). The missile has an ogive forebody with a 20% blunt nose, a moment reference location at  $L/2$ , and a body diameter that is 10% of the total body length. Wind-tunnel tests were conducted at  $M_\infty = 2.01$ ,  $Re = 2 \times 10^6$  per foot, and angles of attack ranging from  $0$  to  $30$  deg. In accordance with Ref. 8, the

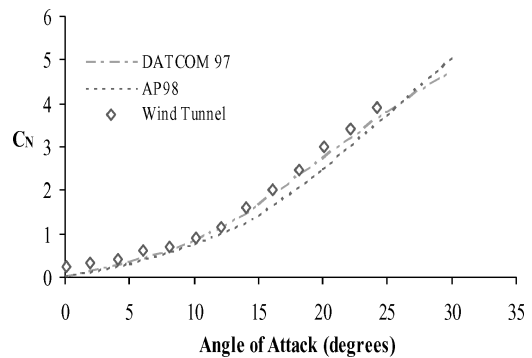


Fig. 17  $C_N$  vs  $\alpha$ ,  $M_\infty = 2.01$ .

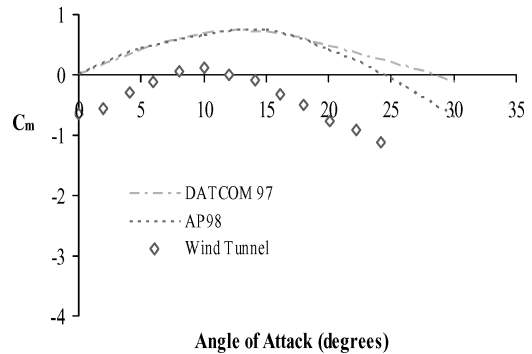


Fig. 18  $C_m$  vs  $\alpha$ ,  $M_\infty = 2.01$ .

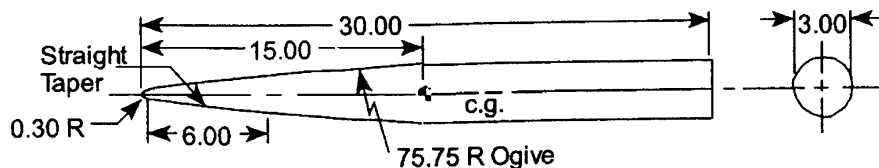


Fig. 16 Body-alone configuration.<sup>9,10</sup>

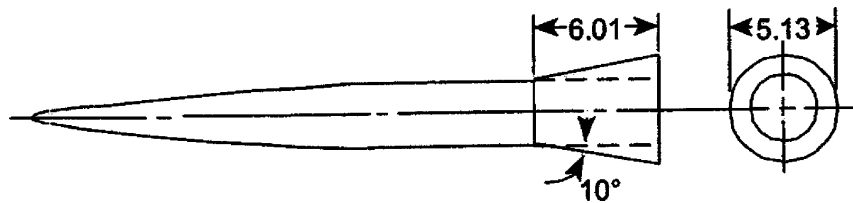


Fig. 19 Body with 10-deg flare afterbody configuration.<sup>10</sup>

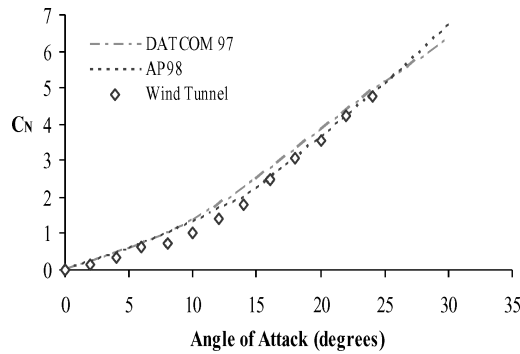


Fig. 20  $C_N$  vs  $\alpha$ ,  $M_\infty = 2.01$ .

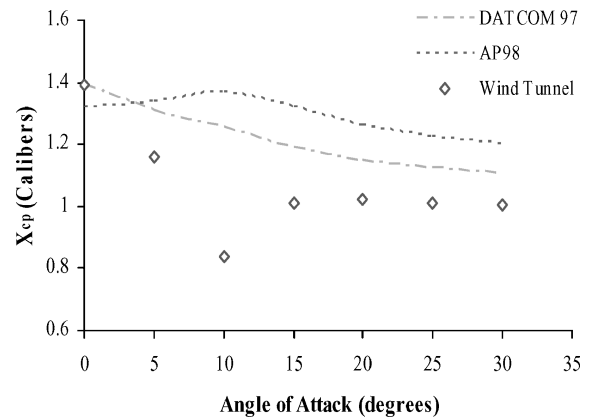


Fig. 22  $X_{CP}$  location vs  $\alpha$ ,  $M_\infty = 2.01$ .

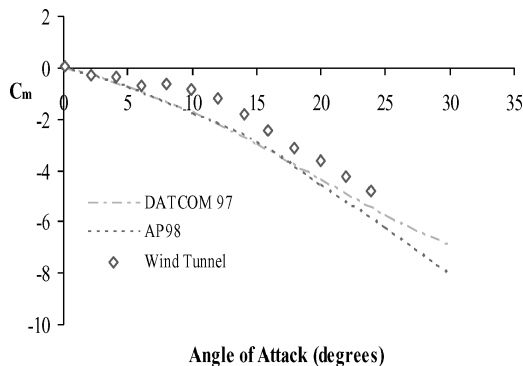


Fig. 21  $C_m$  vs  $\alpha$ ,  $M_\infty = 2.01$ .

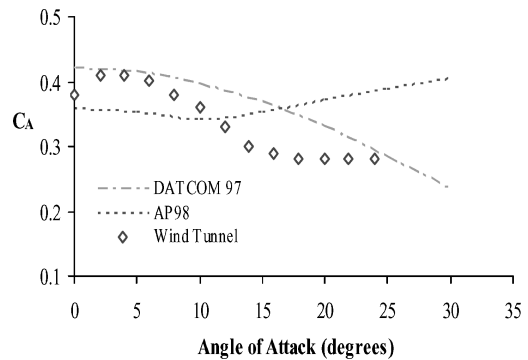


Fig. 23  $C_A$  vs  $\alpha$ ,  $M_\infty = 2.01$ .

tests were conducted at a simulated zero-base-drag condition with a naturally transitioning boundary layer.

The experimental data shown in Figs. 17 and 18 are not indicative of an axisymmetric missile because of the negative pitching moment and nonzero normal-force coefficient value at zero angle of attack. This probably indicates that the data are biased. Though the trend of the data is modeled accurately, error calculations are inconclusive for this case. However, it can be concluded that both codes follow the trend of the wind-tunnel data for the aerodynamic coefficients for this configuration.

#### D. Case 4: Body with 10-deg Flare Afterbody Configuration

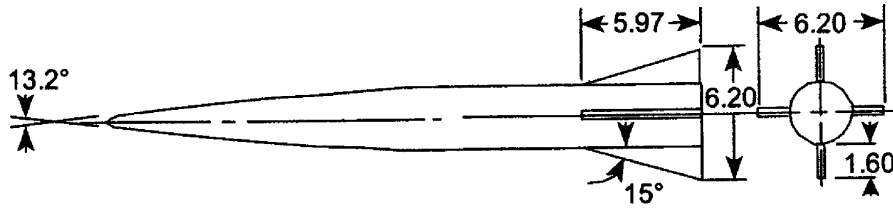
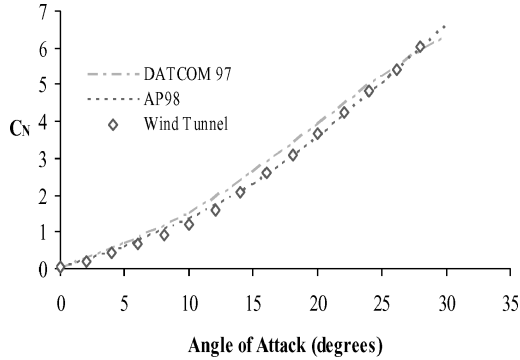
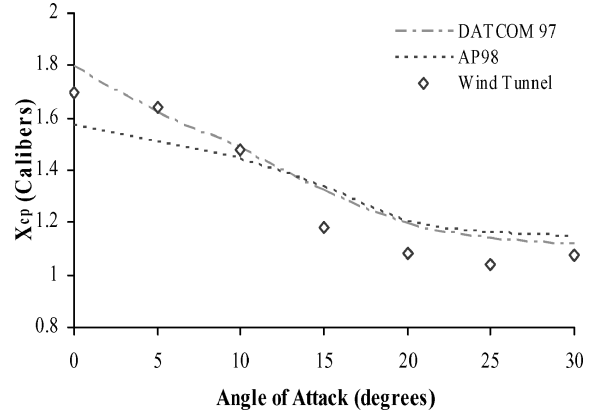
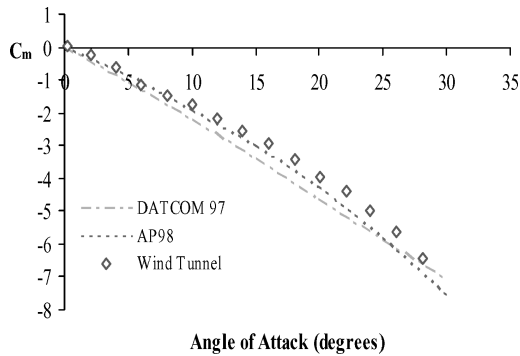
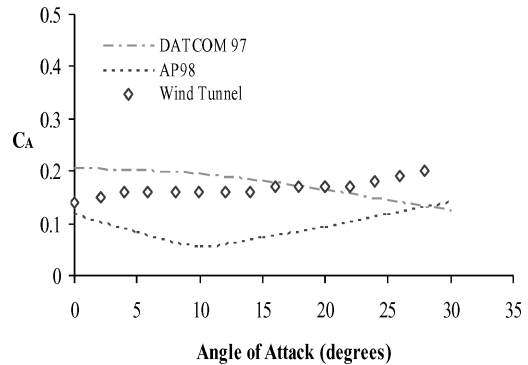
The fourth configuration evaluated is a variation of case 3. The missile, with an additional 10-deg afterbody flare, is shown in Fig. 19. The dimensions of this flare are shown in the figure, with the base diameter increasing, creating a forebody, centerbody, and afterbody arrangement. All other geometric data and flight conditions remain the same, including the zero-base-drag condition, and the boundary-layer stipulations from Ref. 10.

The results are shown in Figs. 20–23. The data in Fig. 20 show minimal discrepancy in normal force, with a 13% error for Missile

DATCOM and 10% for AP98. This larger than expected error is caused by a dip in the wind-tunnel data between approximately 5- and 15-deg angle of attack. Similarly, predicted pitching-moment coefficients from both DATCOM and AP98 follow the trend of the experimental data. The  $X_{CP}$  locations are shown in Fig. 22. Both codes follow the trend of the experimental data but do not model the sudden change in  $X_{CP}$  at 10-deg angle of attack. The axial-force coefficients in Fig. 23 suggest again the inherent difficulty in predicting axial force. For a missile with body flare of this type, DATCOM more closely follows the trend of the wind-tunnel axial force.

#### E. Case 5: Body-Tail Configuration

Another variation of case 3 is shown in Fig. 24. The body-tail configuration has four tail fins, arranged in a cruciform geometry, with constant thickness to the tip. The fins have a leading-edge sweep angle of 75 deg. The airfoil data for the tail fins were described in the reference as “flat plates with rounded leading edges and blunt trailing edges.”<sup>9,10</sup> The configuration was modeled with zero base drag, and all other geometric details, flight conditions, and

Fig. 24 Body-tail configuration.<sup>10</sup>Fig. 25  $C_N$  vs  $\alpha$ ,  $M_\infty = 2.01$ .Fig. 27  $X_{CP}$  location vs  $\alpha$ ,  $M_\infty = 2.01$ .Fig. 26  $C_m$  vs  $\alpha$ ,  $M_\infty = 2.01$ .Fig. 28  $C_A$  vs  $\alpha$ ,  $M_\infty = 2.01$ .

boundary-layer conditions remained the same as the preceding two cases.

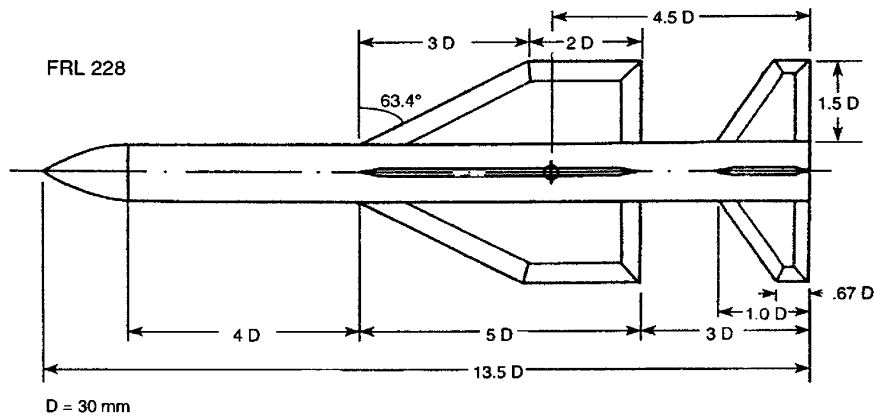
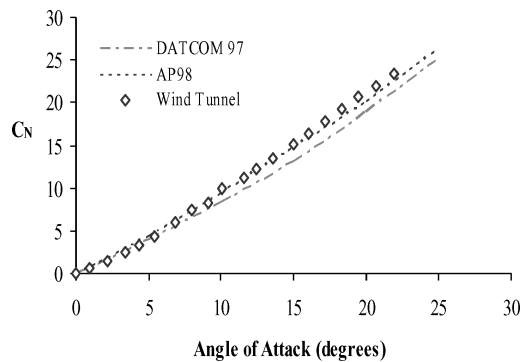
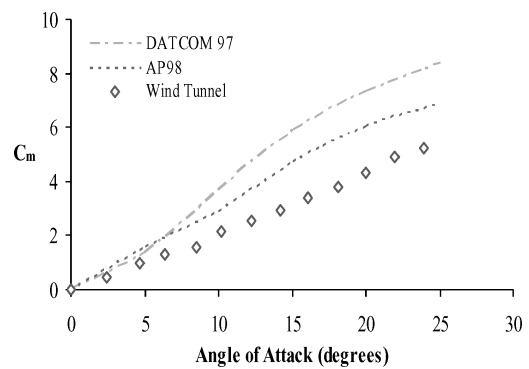
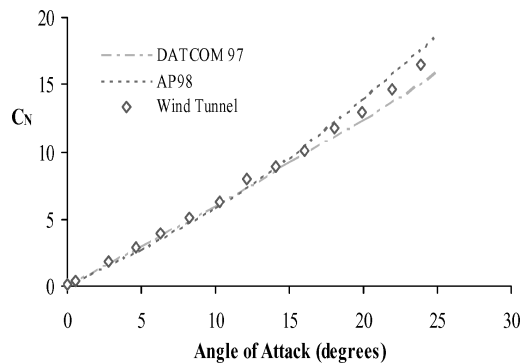
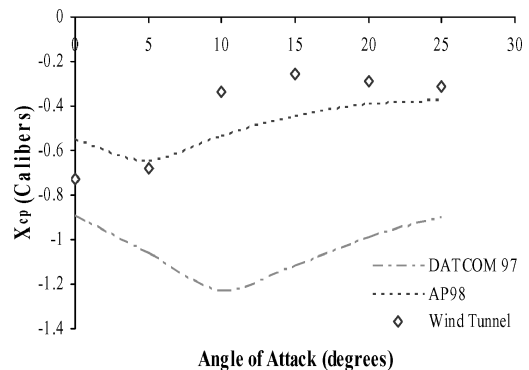
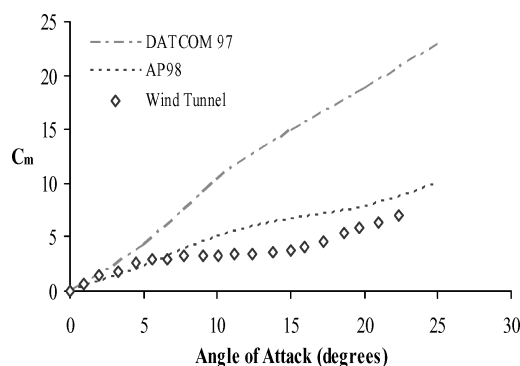
The results are shown in Figs. 25–28. The results for normal-force coefficients are predicted with an 11% error for Missile DATCOM and 6% error for AP98. Pitching-moment coefficient results follow the experimental data closely with an 11% error for DATCOM and a 4% error for AP98. As shown in Fig. 27, center-of-pressure locations are predicted with minimal error. The maximum error calculated is less than 1% for DATCOM and 2% for AP98 at any given angle of attack. For axial force, shown in Fig. 28, AP98 follows the trend of the wind-tunnel data above approximately 10-deg angle of attack; however, both codes show difficulty in predicting axial force for this case.

#### F. Case 6: Body-Wing-Tail Configuration

The next missile modeled for comparison is a high-aspect-ratio body-wing-tail configuration.<sup>10,11</sup> Shown in Fig. 29, the missile has a 1.5-caliber tangent-ogive nose. The wings have a hexagonal double-wedge airfoil, a leading-edge sweep angle of 63.4 deg, a wedge angle of 15 deg, and a thickness-to-chord ratio of 0.0178. The tail fins have a leading-edge sweep angle of 33.69 deg, with a wedge angle of 20 deg. The tail fins also have a hexagonal airfoil with

a thickness-to-chord ratio of 0.05. Both fin sets were assumed to have a constant tapering thickness to the tip. The tail-fin root chord, shown in Fig. 29, is determined from Ref. 11 to be  $1.67 \cdot D$ . The flight conditions this case was modeled under include an angle-of-attack range of 0–25 deg, Mach numbers 1.42 and 3.08, with full base drag, a naturally transitioning boundary layer, and a Reynolds number of  $2 \times 10^6$  per foot.

Figures 30 and 31 show that the normal-force coefficient results are in agreement with the wind-tunnel data. DATCOM predicted normal force with errors of 7 and 3% for Mach 1.42 and 3.08, respectively. AP98 errors were 5 and 7% for Mach 1.42 and 3.08, respectively. The predicted pitching-moment coefficients, in Figs. 32 and 33, show variability especially with the results of DATCOM. In Fig. 34 the center-of-pressure location predicted by DATCOM is closer to the nose than that predicted by AP98. This location produces a larger moment arm, which explains the large discrepancy in pitching-moment coefficient. These results show a possible difficulty in DATCOM's predicted center-of-pressure location for this type of configuration. Given the results shown in Figs. 32–34, it can be concluded for this case study that AP98 predicts more accurate pitching moments, along with center-of-pressure location for this type of configuration at these flight conditions.

Fig. 29 Wing-body-tail configuration.<sup>10,11</sup>Fig. 30  $C_N$  vs  $\alpha$ ,  $M_\infty = 1.42$ ,  $\phi = 0$  deg.Fig. 33  $C_m$  vs  $\alpha$ ,  $M_\infty = 3.08$ ,  $\phi = 0$  deg.Fig. 31  $C_N$  vs  $\alpha$ ,  $M_\infty = 3.08$ ,  $\phi = 0$  deg.Fig. 34  $X_{CP}$  location vs  $\alpha$ ,  $M_\infty = 1.42$ ,  $\phi = 0$  deg.Fig. 32  $C_m$  vs  $\alpha$ ,  $M_\infty = 1.42$ ,  $\phi = 0$  deg.

#### IV. Conclusions

This study was conducted to validate the results produced by two semi-empirical aerodynamic prediction codes, NSWC/DD AP98 and USAF Missile DATCOM (97 version), for various missile configurations including body-alone, body-tail, body-with-flare, and body-wing-tail missiles.

For the configurations detailed in this paper, these case studies show normal-force prediction for both codes to have minimal error.

Both Missile DATCOM and AP98 had discrepancies in pitching-moment coefficient prediction with case 1; however, Missile DATCOM more closely followed the trend of the wind-tunnel data. For body-tail configurations, the results show predicted pitching-moment coefficients to be accurate. In the body-wing-tail configuration of case 6, AP98 more closely followed the trend of the experimental data for pitching moment, which resulted from a more accurately predicted  $X_{CP}$ .

Axial force is one of the most difficult aerodynamic forces to accurately predict. For the body-wing-tail configuration in case 1, AP98



results show the code's capability in predicting axial force within  $\pm 10\%$  error, while error for DATCOM was 12%. For the body-with-flare configuration in case 4, DATCOM more closely followed the trend of the wind-tunnel data. Overall, both codes showed difficulty in predicting accurate axial-force data.

For the body-wing-tail configuration in case 6, DATCOM shows a possible difficulty in predicting  $X_{CP}$ . This possible prediction problem can easily be adjusted by an analytical correction factor, but this is beyond the scope of this paper. Overall, both codes predicted center-of-pressure locations that followed the trends of the experimental data with minimal errors.

It can be expected that for similar configurations and flight conditions both codes will produce results that closely follow the trends presented in this report.

### Acknowledgments

The authors thank F. Moore and W. Blake for their consultations. Their expertise was instrumental in the development of this study.

### References

- <sup>1</sup>Blake, W. B., *Missile DATCOM: User's Manual—1997 Fortran 90 Revision*, U.S. Air Force Research Lab./Air Vehicles Directorate, Wright-Patterson AFB, OH, Feb. 1998.
- <sup>2</sup>Moore, F. G., Hymer, T. C., and Downs, C., *User's Guide for an Interactive Personal Computer Interface for the 1998 Aeroprediction Code (AP98)*, U.S. Naval Surface Warfare Center, Dahlgren Div., Dahlgren, VA, June 1998.
- <sup>3</sup>Moore, F. G., *Combination AP98 Theory and User's Course Manual*, Aeroprediction Inc. (API), King George, VA, 2001, pp. 29–34.
- <sup>4</sup>Miller, M. S., and Packard, J. D., "Assessment of Engineering Level Codes for Missile Aerodynamic Design and Analysis," AIAA Paper 2000-4590, Aug. 2000.
- <sup>5</sup>Zona, R., "Aerodynamic Predictions, Comparisons, and Validations Using Missile DATCOM," Technology Service Corp., W233-001/rlz, Silver Spring, MD, Sept. 2001.
- <sup>6</sup>Chapra, S. C., *Numerical Methods for Engineers*, 3rd ed., McGraw-Hill, New York, 1998, pp. 425, 426.
- <sup>7</sup>Monta, W. J., "Supersonic Aerodynamic Characteristics of a Sparrow III Type Missile Model with Wing Controls and Comparison with Existing Tail-Control Results," NASA TP S-1078, Nov. 1977.
- <sup>8</sup>Oktay, E., Alemdaroğlu, N., Tarhan, R., Champigny, P., and d'Espiney, P., "Euler and Navier-Stokes Solutions for Missiles at High Angles of Attack," *Journal of Spacecraft and Rockets*, Vol. 36, No. 6, 1999, pp. 850–858.
- <sup>9</sup>Robinson, R. B., "Wind-Tunnel Investigation at a Mach Number of 2.01 of the Aerodynamic Characteristics in Combined Angles of Attack and Sideslip of Several Hypersonic Missile Configurations with Various Canard Controls," NACA RM L58A21, March 1958.
- <sup>10</sup>Moore, F. G., *Approximate Methods for Weapon Aerodynamics*, edited by P. Zarchan, Vol. 186, Progress in Astronautics and Aeronautics, AIAA, Reston, VA, 2000, pp. 270–290.
- <sup>11</sup>Gudmundson, S. E., and Torngren, L., "Supersonic and Transonic Wind Tunnel Tests on a Slender Ogive-Cylinder Body Single and in Combination with Cruciform Wings and Tails of Different Sizes," National Technical Information Service, 093375 and 093376, U.S. Dept. of Commerce, Washington, DC, April 1972.

M. Miller  
Associate Editor